Syntheses and Physicochemical Properties of Polycyano-Substituted Buta-1,3-dienylidene- and Allenylidene-Bridged Diiron Complexes

Michel Etienne,*[†,‡] Jean Talarmin,[†] and Loïc Toupet[§]

URA CNRS 322, Chimie, Electrochimie et Photochimie Moléculaires, Université de Bretagne Occidentale,
29287 Brest Cedex, France, Laboratoire de Chimie de Coordination du CNRS,
205 Route de Narbonne, 31077 Toulouse Cedex, France, and URA CNRS 804, Groupe
Matière Condensée et Matériaux, Université de Rennes I, Beaulieu, 35042 Rennes Cedex, France

Received November 13, 1991

Treatment of the (μ-ethenylidene)diiron complexes $Cp_2Fe_2L_2(\mu\text{-}CO)(\mu\text{-}C{=}CH_2)$ (L = CO (**1a**); L_2 = dppe (**1b**), dppm (**1c**)) with tetracyanoethylene (tcne) results in the formation of the μ-3,4,4-tricyanobuta-1,3-dienylidene complexes $Cp_2Fe_2L_2(\mu\text{-}CO)[\mu\text{-}C{=}CHC(CN){=}(CN)_2]$ (**2a–c**) and the μ-3,3-dicyanoallenylidene complexes $Cp_2Fe_2L_2(\mu\text{-}CO)[\mu\text{-}C{=}C{=}C(CN)_2]$ (**3b,c**). The tricyanobutadienylidene ligand is shown to be a very good π-acceptor on the basis of infrared and NMR data. An X-ray diffraction analysis has been carried out on complex **2a** (L = CO) (monoclinic, space group $P2_1/c$, a = 11.621 (4) Å, b = 7.904 (4) Å, c = 20.546 (5) Å, β = 94.00 (2)°, Z = 4, R = 0.032, R_w = 0.031 for 2025 reflections with $I > 3\sigma(I)$). The bridging tricyanobutadienylidene ligand is planar and exhibits extensive electron delocalization. Complexes **2a** (L = CO) and **2b** (L_2 = dppe) strongly absorb light in the visible region (**2a**, λ_{max} = 476 nm, ϵ = 25 500 L mol^{-1} cm^{-1}; **2b**, λ_{max} = 539 nm, ϵ = 25 700 L mol^{-1} cm^{-1}). These absorptions are proposed to be mainly $\pi \rightarrow \pi^*$ μ-tricyanobutadienylidene ligand based. More or less restricted rotation about the C_α–C_β bond of the μ-tricyanobutadienylidene ligand in **2a,b** is observed by dynamic NMR studies. The difference for the energy barriers (**2a**, $\Delta G^{\ddagger}{}_{298}$ = 16 ± 1 kcal mol^{-1}; **2b**, $\Delta G^{\ddagger}{}_{211}$ = 10 ± 0.2 kcal mol^{-1}) is consistent with the stabilization of a dipolar mesomeric form, as suggested by the X-ray data. The μ-3,3-dicyanoallenylidene complexes (**3b,c**) have been characterized spectroscopically and by X-ray diffraction analysis (**3b**·CH_2Cl_2, monoclinic, space group $C2/c$, a = 22.222 (8) Å, b = 13.677 (5) Å, c = 25.746 (9) Å, β = 103.44 (3) Å, Z = 8, R = 0.048, R_w = 0.045 for 3550 reflections with $I > 2\sigma(I)$). The μ-allenylidene ligand has a short C_α–C_β double bond (C(36)–C(37) = 1.285 (5) Å) and a normal C_β–C_γ double bond (C(37)–C(38) = 1.345 (6) Å). Cyclic voltammetry data and ESR and ^{1}H NMR studies on reaction mixtures of **1a,b** and tcne allow a reaction mechanism to be proposed. Protonation of the μ-allenylidene complex **3b** occurs reversibly at C_β. The cationic μ-(2,2-dicyanovinyl)carbyne complex $Cp_2Fe_2(\mu\text{-}CO)(\mu\text{-}dppe)[\mu\text{-}CCH{=}C(CN)_2]^+BF_4^-$ (**4b**) has been isolated and characterized spectroscopically.

Introduction

There is now good experimental and theoretical evidence that alkenylidenediiron complexes of the type $[CpFe(CO)]_2(\mu\text{-}CO)(\mu\text{-}C{=}CHR)$ may be viewed as 1,1-dimetalated electron-rich olefins. Diazomethane[1] as well as substituted diazo compounds[2] react to give μ-cyclopropylidene complexes that rearrange to μ-allene complexes upon photolysis. This reaction is also known for the ruthenium analogues.[3] These results have been analyzed via Fenske–Hall calculations.[4] The reactive site in these cases is indeed an occupied molecular orbital, that of the π-system of the $C{=}CH_2$ unit, which is not involved in the bonding with the bimetallic moiety and which is energetically and spatially exposed. We have previously found[5] that it was possible to observe a [3 + 2] type of cycloaddition between tetracyanoethylene (tcne) and the isopropyl-substituted μ-alkenylidene complex $[CpFe(CO)]_2(\mu\text{-}CO)(\mu\text{-}C{=}CHCH(CH_3)_2)$ leading to the μ-cyclopentylidene complex $[CpFe(CO)]_2(\mu\text{-}CO)[\mu\text{-}CCH_2C(CH_3)_2C(CN)_2C(CN)_2]$. Pursuing the analogy and considering that tcne[6,7] reacts with electron-rich alkenes such as vinyl ethers to give [2 + 2] cycloadducts, we have examined the behavior of simple (μ-ethenylidene)diiron complexes in the presence of tcne in the hope of forming μ-cyclobutylidene complexes. Until now, we have not observed any complex of that type but original rearranged compounds have been obtained from these reactions. We report here the preparation and full characterization of cyano-substituted (μ-buta-1,3-dienylidene)- and (μ-allenylidene)diiron complexes derived from $[CpFe(CO)]_2(\mu\text{-}CO)(\mu\text{-}C{=}CH_2)$ (**1a**) and $Cp_2Fe_2(\mu\text{-}CO)(\mu\text{-}P\text{-}P)(\mu\text{-}C{=}CH_2)$ (P-P = 1,2-bis(diphenylphosphino)ethane = dppe (**1b**); P-P = bis(diphenylphosphino)methane = dppm (**1c**)). Interesting physicochemical properties and mechanistic studies are also included. Aspects of this chemistry have already appeared.[8,9]

Results and Discussion

Syntheses of Starting Materials. The diphosphine-bridged (μ-ethenylidene)diiron complexes $Cp_2Fe_2(\mu\text{-}dppe)(\mu\text{-}C{=}CH_2)$ (**1b**) and $Cp_2Fe_2(\mu\text{-}CO)(\mu\text{-}dppm)(\mu\text{-}C{=}CH_2)$ (**1c**) are obtained from the μ-ethenylidene complex[10] $[CpFe(CO)]_2(\mu\text{-}CO)(\mu\text{-}C{=}CH_2)$ (**1a**) and an excess of the appropriate diphosphine in refluxing toluene for 36 h.

[†] URA CNRS 322.

[‡] Present address: Laboratoire de Chimie de Coordination du CNRS.

[§] URA CNRS 804.

(1) (a) Hoel, E. L.; Ansell, G. B.; Leta, S. *Organometallics* **1984**, *3*, 1633. (b) Hoel, E. L.; Ansell, G. B.; Leta, S. *Ibid.* **1986**, *5*, 585. (c) Hoel, E. L. *Ibid.* **1986**, *5*, 587.

(2) (a) Casey, C. P.; Austin, E. A. *Organometallics* **1986**, *5*, 584. (b) Casey, C. P.; Austin, E. A. *J. Am. Chem. Soc.* **1988**, *110*, 7106.

(3) Lewandos, G. S.; Doherty, N. M.; Knox, S. A. R.; MacPherson, K. A.; Orpen, A. G. *Polyhedron* **1988**, *7*, 837.

(4) Bursten, B. E.; Cayton, R. H. *J. Am. Chem. Soc.* **1986**, *108*, 8241.

(5) Etienne, M.; Toupet, L. *Organometallics* **1990**, *9*, 2023.

(6) Huisgen, R. *Acc. Chem. Res.* **1977**, *10*, 117, 199.

(7) Reviews on tcne chemistry: Fatiadi, A. J. *Synthesis* **1986**, 249; **1987**, 749; **1987**, 959. See also: *The chemistry of the cyano group*; Rappoport, Z., Patai, S., Eds.; Wiley: London, 1970.

(8) Etienne, M.; Toupet, L. *J. Organomet. Chem.* **1988**, *344*, C19.

(9) Etienne, M.; Toupet, L. *J. Chem. Soc., Chem. Commun.* **1989**, 1110.

(10) Dawkins, G. M.; Green, M.; Jeffrey, J. C.; Sambale, C.; Stone, F. G. A. *J. Chem. Soc., Dalton Trans.* **1983**, 499.

Typical yields are in the range of 70–80%. The compounds are obtained as brown-green powders and can be recrystallized from dichloromethane/hexane mixtures to give dark green crystals (the same kind of procedure was used previously to prepare diphosphine-bridged derivatives of the type $Cp_2Fe_2(\mu\text{-}CO)_2(\mu\text{-}L)$ (L = diphosphines, etc.)[11] from $[CpFe(CO)_2]_2$). They have been characterized by elemental analyses and infrared and ^1H, ^{31}P, and ^{13}C NMR spectroscopies. The salient features of the infrared spectra of **1b**,**c** are the absence of any terminal carbonyl stretches and the fact that the bridging carbonyl stretch is shifted to lower frequencies by ca. 100 cm^{-1} compared to that for **1a**, which is expected upon diphosphine substitution. In the ^1H NMR spectra, the methylene protons appear as a triplet for both **1b** and **1c**, due to the coupling with the phosphorus atoms ($J_{PH} \sim 3$ Hz). In the ^{13}C NMR of **1b**, the bridging carbon C_α of the ethenylidene and carbonyl ligands also gives a triplet because of the same type of coupling. The C_β carbon of the μ-ethenylidene ligand gives a triplet at δ 123.6 with $J_{CH} = 155$ Hz. The cyclic voltammetry and UV visible absorption spectrum of **1b** are presented below in the proper section. The main conclusion is that, because of the diphosphine substitution, complexes **1b** and **1c** are more electron-rich than complex **1a**.

Reaction of $[CpFe(CO)]_2(\mu\text{-}CO)(\mu\text{-}C{=}CH_2)$ (1a) with tcne. As described previously,[8] the reaction between the μ-ethenylidene complex **1a** and tcne in toluene leads to the isolation of highly colored crystals of the (μ-3,4,4-tricyanobuta-1,3-dienylidene)diiron complex *cis*-$[CpFe(CO)]_2(\mu\text{-}CO)[\mu\text{-}C{=}CHC(CN){=}C(CN)_2]$ (**2a**) in ca. 70% yield (eq 1). Complex **2a** was characterized by elemental analysis as well as by infrared and ^1H and ^{13}C NMR spectroscopies and X-ray diffraction. When the reaction was followed by ^1H NMR, other products were seen but could not be isolated. Hydrogen cyanide was detected in the gas phase above the reaction mixture from its rotation–vibration spectrum.[12]

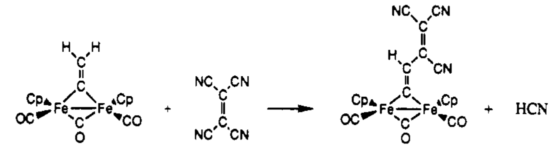

(1)

1a **2a**

The most noticeable features in the infrared spectrum of **2a** (CH_2Cl_2 solution) are the high frequencies of the carbonyl absorption bands. The terminal stretches are observed at 2015 (s) and 1980 (m) cm^{-1} (indicating a cis arrangement), and the bridging carbonyl gives a broader band at 1815 cm^{-1}. For **1a** these bands are observed at 1998, 1963, and 1804 cm^{-1}.[10] A somewhat intense nitrile stretch is observed at 2205 cm^{-1}, and strong bands attributed to double carbon–carbon bond stretches are also present at 1470 and 1460 cm^{-1}. The intensity of these bands is a direct consequence of conjugation and electronic delocalization over the ligand.

The ^{13}C NMR data are also a reliable diagnostic. The bridging carbon C_α of the butadienylidene ligand is highly deshielded at δ 343, and the other carbons of the bridge are found at δ 139 ($J_{CH} = 159$ Hz) for C_β, δ 132 for C_γ, and ultimately, highly shielded, at δ 74 for C_δ. In the acetone-d_6 room-temperature ^1H NMR spectrum, the cyclopentadienyl protons appear as a broad resonance: this is analyzed below as a restricted rotation of the bridging ligand about the C_α–C_β bond. At 251 K two cyclopentadienyl proton signals are observed at δ 5.39 and 5.36, and the β proton of the bridging ligand appears at δ 8.97, somewhat shifted downfield (δ 7 in **1a**).

Scheme I

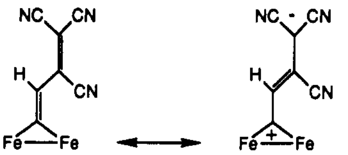

Taken altogether, these spectroscopic features indicate that the 3,4,4-tricyanobuta-1,3-dienylidene ligand is a strong π-acceptor and a strong electron-withdrawing group with extensive electron delocalization all over it. We have previously synthesized[13] a series of mono- and dicyano-substituted (μ-buta-1,3-dienylidene)diiron complexes of the type $[CpFe(CO)]_2(\mu\text{-}CO)[\mu\text{-}C{=}CR_1CR_2{=}C(CN)H]$ (R_1, R_2 = H, alkyl; R_1 = H, R_2 = CN), and it is now obvious that when the number of cyano groups increases, the π-accepting properties of the bridging ligand increase: the carbonyl stretches shift to higher frequencies and the C_α and C_δ are respectively more deshielded and more shielded. It is also noteworthy that, even upon standing in solution for 15 h in $CDCl_3$ in an NMR probe, no cis–trans isomerization about the iron–iron bond occurred, the cis isomer of **2a** remaining unchanged. This indicates of strong preference for a bridging position of this powerful π-acceptor ligand as expected. The X-ray structure of **2a** (see below) also reveals that the C_β–C_γ bond (1.406 (5) Å) contains a substantial amount of double character. Thus, all the data indicate that a dipolar mesomeric form (Scheme I) with a positive charge on the C_α carbon, stabilized by the electron-rich diiron moiety, and a negative charge on the C_δ carbon, stabilized by the electron-withdrawing nitrile groups, is an important contribution in the description of the bonding in complex **2a**. Also remarkable is that complex **2a** has a very intense golden red color. Its UV–visible absorption spectrum is discussed below.

Reaction of $Cp_2Fe_2(\mu\text{-}CO)(\mu\text{-}P\text{-}P)(\mu\text{-}C{=}CH_2)$ (P-P = dppe (1b); P-P = dppm (1c)) with tcne. When the green-brown μ-ethenylidene complexes **1b** or **1c** and tcne are dissolved in dichloromethane, a deep violet color instantaneously develops.[9] After 30 min, the reaction mixture was chromatographed on a silica gel column.

The first, less abundant, green band yields (μ-3,3-dicyanoallenylidene)diiron complexes. The second, partially overlapping, violet band gives the diphosphine bridged congeners of **2a**, namely the μ-3,4,4-tricyanobuta-1,3-dienylidene complexes $Cp_2Fe_2(\mu\text{-}CO)(\mu\text{-}P\text{-}P)[\mu\text{-}C{=}CHC(CN){=}C(CN)_2]$ (P-P = dppe (**2b**); P-P = dppm (**2c**)), in ca. 60–70% yield after recrystallization from dichloromethane/hexanes (eq 2). Both compounds exhibit the same qualitative spectroscopic features previously noted for **2a**. The bridging carbonyl stretches now appear at 1740 cm^{-1}, to be compared with 1705 cm^{-1} for **1b** and **1c**. In the room-temperature ^1H NMR of both **2b** and **2c**, the H_β proton of the bridge appear as a triplet due to the coupling with the phosphorus atoms respectively at δ 9.39 (J_{PH} = 1.9 Hz) and δ 9.32 (J_{PH} = 2.2 Hz). In the ^{13}C NMR spectra, the bridging carbons give signals at δ 379 appearing as triplets (16–17 Hz) due to coupling with the phosphorus atoms. Again the remote C_δ carbon of the bridge is highly shielded at δ 58. Hence, even if the NMR chemical shifts

---

(11) Haines, R. J.; DuPreez, A. L. *J. Organomet. Chem.* **1970**, *21*, 181.

(12) Cole, A. R. H. *Tables of wavenumbers for the calibration of infrared spectrometers*; IUPAC, Pergamon Press: Oxford, England, 1977; p 8.

(13) Etienne, M.; Guerchais, J. E. *J. Chem. Soc., Dalton Trans.* **1989**, 2187.

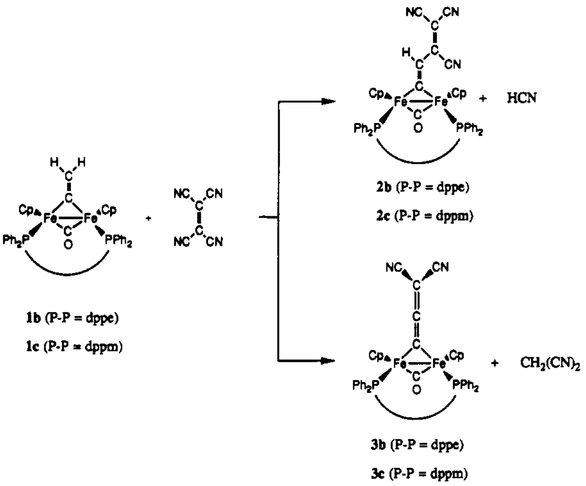

(2)

are not only influenced by the net charge at carbon (the nitrile groups shield the α carbon as a result of magnetic anisotropy), it seems reasonable to conclude that the dipolar mesomeric form (Scheme I) is even more important for these diphosphine-bridged complexes **2b,c** than it was for **2a**. This assumption is supported by variable-temperature NMR studies described below. Also analyzed below is the intense violet color that characterizes these complexes.

From the first green band, the rare (μ-3,3-dicyanoallenylidene)diiron complexes $Cp_2Fe_2(\mu\text{-}CO)(\mu\text{-}P\text{-}P)[\mu\text{-}C{=}C{=}C(CN)_2]$ (P-P = dppe (**3b**); P-P = dppm (**3c**)) were isolated in respectively 17% and 10% yield. Malononitrile $CH_2(CN)_2$ has been identified by its ^1H NMR spectrum as the other product of this reaction. A X-ray crystal structure of **3b** has been obtained (see below). The infrared spectra of these μ-dicyanoallenylidene complexes exhibit bridging carbonyl bands between 1735 and 1740 cm^{-1} as well as two sharp nitrile stretches at 2200 and 2190 cm^{-1}. The most interesting feature of these spectra is the presence of a band at 1837 cm^{-1} (for **3b**) or 1835 cm^{-1} (for **3c**). This absorption is attributed to the vibration of the allene-like bridging ligand. This vibration is also observed in other rare μ-σ,σ-allenylidene complexes[14] as well as in mononuclear allenylidene complexes.[15] We note that the wavenumbers are higher for mononuclear complexes (from 1920 to 1961 cm^{-1}) than for bimetallic compounds (from 1835 to 1907 cm^{-1}). Quite interesting are the ^{13}C NMR spectra of **3b** and **3c**. The bridging C_α carbons are observed as triplets because of the coupling with the phosphorus atoms (J_{PC} = 17 Hz for **3b**; J_{PC} = 19 Hz for **3c**), at δ 173.1 and 176.0 for **3b,c**, respectively. The C_β carbons give non-phosphorus-coupled resonances at δ 201.2 and 199.3 for **3b,c**, respectively. The C_γ carbons are highly shielded at δ 39.5 and 40.4 for **3b,c**, respectively.

Crystal Structure of 2a. Results of the X-ray analysis are summarized in Table I and in the Experimental Section. Positional parameters and bond lengths and angles are provided in Tables II and III, and a perspective view of the molecule is depicted in Figure 1.

The overall geometry, with a cis disposition of the CpFe(CO) units bridged by a carbonyl and a μ-3,4,4-tricyanobuta-1,3-dienylidene group, is that observed for any complex of the type $[CpFe(CO)]_2(\mu\text{-}CO)(\mu\text{-}L)$.[1,16] The

Table I. Crystal Data and Experimental Details of the X-ray Diffraction Analyses

	2a	3b
formula	$Fe_2O_3N_3C_{20}H_{11}$	$Fe_2P_2C_{42}H_{34}ON_2$, CH_2Cl_2
mol wt	469	840.3
cryst syst	monoclinic	monoclinic
space group	$P2_1/c$	$C2/c$
a, Å	11.621 (4)	22.222 (8)
b, Å	7.904 (4)	13.677 (5)
c, Å	20.546 (5)	25.746 (9)
β, deg	94.00 (2)	103.44 (3)
V, Å^3	1182.6 (7)	7610.4 (8)
Z	4	8
cryst dimens, mm	0.15 × 0.15 × 0.20	0.12 × 0.22 × 0.27
D(calcd), Mg m^{-3}	1.65	1.467
λ(Mo Kα) Å	0.71073	0.71073
abs coeff, cm^{-1}	14.8	10.2
F(000)	912	3456
T, K	296	296
scan type	$\omega/2\theta = 1$	$\omega/2\theta = 1$
2θ max, deg	50	50
scan speed	var (t_{max} = 60 s)	var (t_{max} = 60 s)
data collcd	$0 \le h \le 13$ $0 \le k \le 9$ $-24 \le l \le 24$	$0 < h \le 26$ $0 \le k \le 16$ $-30 \le l \le 30$
no. of reflns	3521	6786
no. of indep reflns	2025 ($I > 3\sigma(I)$)	3550 ($I > 2\sigma(I)$)
no. of variables	286	559
R	0.032	0.048
R_w	0.031	0.045
S_w, goodness of fit	1.27	1.52
Δe, final electron density, e Å^{-3}	0.28	0.45

Table II. Positional Parameters and Their Estimated Standard Deviations for 2a[a]

atom	x	y	z	B, Å^2
Fe1	0.64008 (4)	0.20074 (7)	0.13171 (2)	3.32 (1)
Fe2	0.76295 (4)	0.13533 (7)	0.23353 (2)	3.40 (1)
O1	0.5291 (2)	0.2396 (5)	0.2541 (2)	7.03 (9)
O2	0.6509 (4)	0.5661 (4)	0.1277 (2)	8.8 (1)
O3	0.8369 (3)	0.4734 (4)	0.2703 (2)	7.47 (9)
N1	0.7709 (3)	0.4130 (5)	−0.0144 (2)	6.2 (1)
N2	1.0576 (4)	0.3043 (6)	−0.0909 (2)	7.1 (1)
N3	1.1926 (3)	0.0534 (7)	0.0841 (2)	8.1 (1)
C1	0.6073 (3)	0.2087 (6)	0.2237 (2)	4.36 (9)
C2	0.6481 (4)	0.4231 (6)	0.1302 (2)	5.0 (1)
C3	0.8072 (4)	0.3405 (6)	0.2560 (2)	4.7 (1)
C4	0.8004 (3)	0.1829 (4)	0.1475 (2)	3.13 (7)
C5	0.9025 (3)	0.1895 (5)	0.1192 (2)	3.78 (8)
C6	0.9223 (3)	0.2411 (5)	0.0554 (2)	3.88 (8)
C7	0.8344 (3)	0.3347 (5)	0.0169 (2)	4.33 (9)
C8	1.0247 (3)	0.2172 (6)	0.0262 (2)	4.33 (9)
C9	1.0418 (4)	0.2688 (6)	−0.0387 (2)	5.0 (1)
C10	1.1177 (3)	0.1265 (7)	0.0594 (2)	5.5 (1)
C11	0.7142 (4)	−0.0476 (7)	0.3017 (2)	7.1 (1)
C12	0.7394 (4)	−0.1270 (6)	0.2461 (3)	6.5 (1)
C13	0.8525 (4)	−0.0966 (6)	0.2337 (2)	5.8 (1)
C14	0.8979 (4)	0.0082 (7)	0.2834 (2)	6.0 (1)
C15	0.8119 (5)	0.0362 (7)	0.3250 (2)	7.0 (1)
C16	0.5510 (4)	0.1928 (6)	0.0407 (2)	6.2 (1)
C17	0.4765 (4)	0.1600 (8)	0.0877 (3)	8.9 (2)
C18	0.5146 (5)	0.0096 (8)	0.1186 (2)	11.0 (1)
C19	0.6068 (5)	−0.0342 (6)	0.0886 (3)	7.8 (1)
C20	0.6283 (4)	0.0749 (6)	0.0419 (2)	6.1 (1)

[a] B values for anisotropically refined atoms are given in the form of the isotropic equivalent thermal parameter defined as: $(4/3)[a^2B(1,1) + b^2B(2,2) + c^2B(3,3) + ab(\cos\gamma)B(1,2) + ac(\cos\beta)B(1,3) + bc(\cos\alpha)B(2,3)]$.

---

(14) (a) Berke, H. *J. Organomet. Chem.* **1980**, *185*, 75. (b) Kolobova, N. E.; Ivanov, L. L.; Zhvanko, O. S.; Aleksandrov, G. G.; Struchkov, Y. T. *J. Organomet. Chem.* **1982**, *228*, 265. (c) Berke, H.; Härter, P.; Huttner, G.; Zsolnai, L. *Chem. Ber.* **1982**, *115*, 695. (d) Berke, H.; Härter, P.; Huttner, G.; Zsolnai, L. *Chem. Ber.* **1984**, *117*, 3423. (e) Berke, H.; Grössman, V.; Huttner, G.; Zsolnai, L. *Chem. Ber.* **1984**, *117*, 3432.

(15) Recent review on vinylidene- and allenylidenemetal complexes: Bruce, M. I. *Chem. Rev.* **1991**, *91*, 197. See also: Bruce, M. I.; Swincer, A. G. *Adv. Organomet. Chem.* **1983**, *22*, 59.

(16) (a) Orpen, A. G. *J. Chem. Soc., Dalton Trans.* **1983**, 1427. (b) Meyer, B. B.; Riley, P. E.; Davis, R. E. *Inorg. Chem.* **1981**, *20*, 3024. (c) Bryan, R. F.; Greene, P. T.; Newlands, M. J.; Field, D. S. *J. Chem. Soc. A* **1970**, 3068.

Table III. Selected Bond Lengths (Å) and Angles (deg) with Esd's for 2a[a]

	Bond Lengths		
Fe1–Fe2	2.503 (1)	O3–C3	1.139 (5)
Fe1–C1	1.954 (4)	N1–C7	1.128 (5)
Fe1–C2	1.760 (5)	N2–C9	1.136 (5)
Fe1–C4	1.874 (3)	N3–C10	1.135 (6)
Fe2–C1	1.897 (4)	C4–C5	1.358 (5)
Fe2–C3	1.753 (5)	C5–C6	1.406 (5)
Fe2–C4	1.888 (3)	C6–C7	1.451 (6)
Fe1–Ct′	1.745 (5)	C6–C8	1.382 (5)
Fe2–Ct″	1.742 (5)	C8–C9	1.422 (6)
O1–C1	1.165 (4)	C8–C10	1.430 (6)
O2–C2	1.132 (5)		
	Bond Angles		
Fe2–Fe1–C1	48.5 (1)	C4–C5–C6	127.9 (4)
Fe2–Fe1–C2	101.1 (1)	C5–C6–C7	120.1 (3)
Fe2–Fe1–C4	48.5 (1)	C5–C6–C8	124.5 (4)
C1–Fe1–C2	90.0 (2)	C7–C6–C8	115.3 (3)
C1–Fe1–C4	95.4 (2)	N1–C7–C6	176.1 (4)
C2–Fe1–C4	91.4 (2)	C6–C8–C9	123.3 (4)
C1–Fe2–C3	90.3 (2)	C6–C8–C10	120.4 (4)
C1–Fe2–C4	96.9 (2)	C9–C8–C10	116.2 (4)
C3–Fe2–C4	88.8 (2)	N2–C9–C8	177.3 (5)
Fe1–C1–Fe2	81.1 (2)	N3–C10–C8	178.0 (5)
Fe2–C1–O1	141.3 (4)	Fe2–C4–C5	132.4 (3)
Fe1–C1–O1	137.6 (3)	Fe1–C4–C5	144.2 (3)
Fe1–C2–O2	178.0 (4)	Fe1–Fe2–Ct″	136.4 (3)
Fe2–C3–O3	179.3 (4)	Fe2–Fe1–Ct′	134.7 (3)
Fe1–C4–Fe2	83.4 (1)		

[a] Ct^x is the centroid of Cp bonded to Fe*x*.

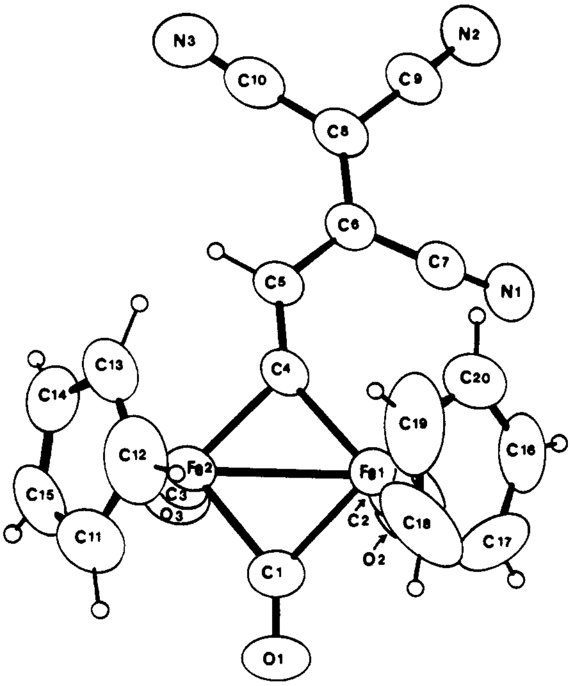

Figure 1. ORTEP plot of complex **2a**.

bridging μ-3,4,4-tricyanobuta-1,3-dienylidene is well defined as a diene, with extensive electronic delocalization: it is planar, and the C_β–C_γ bond length (C5–C6 = 1.406 (5) Å) is typically between that of a single and a double bond and substantially shorter than the C_{sp^2}–C_{sp^2} single bond in butadiene (1.47 Å).[17] The C6–C8 bond length of 1.382 (5) Å is notably elongated when compared to the C_{sp^2}–C_{sp^2} bond of tcne (1.344 (3) Å).[18] The "alkenylidene" C4–C5 bond length is 1.358 (5) Å. This bond length is between that observed in a very electron-poor (μ-2,2-dicyanoethenylidene)diiron complex[19] $[CpFe(CO)]_2(\mu$-$CO)[\mu$-$C{=}C(CN)_2]$ (C_α–C_β = 1.38 (3) Å) and that observed[20] in typical μ-alkenylidene complex $[CpFe(CO)]_2(\mu$-$CO)[\mu$-$C{=}C(Ph)CH_2Ph]$ (C_α–C_β = 1.326 (4) Å). Evidence for very strong π-accepting properties of the ligand and strong bonding interactions with the diiron moiety are found in the following data: the iron–iron bond (Fe1–Fe2 = 2.503 (1) Å) is short (compare to 2.511 (4) and 2.5104 (5) Å for the μ-$C{=}C(CN)_2$ and μ-$C{=}C(Ph)CH_2Ph$ alkenylidene derivatives, respectively,[19,20] and to 2.520 (2) Å for an alkylidene derivative $[CpFe(CO)]_2(\mu$-$CO(\mu$-$CHCH_3)]$[16a,b]), and also short are the iron-bridging carbon (C4) bonds (average Fe–C4 = 1.881 (3) Å, whereas Fe–μ-C is 1.87 (4) and 1.940 (3) Å for the μ-$C{=}C(CN)_2$ and the μ-$C{=}C(Ph)CH_2Ph$ derivatives, respectively[19,20]). The correlation is a larger Fe–μ-C–Fe angle (Fe1–C4–Fe2 = 83.4 (1)° for **2a**; 84 (2) and 80.9 (1)° for the μ-$C{=}C(CN)_2$ and the μ-$C{=}C(Ph)CH_2Ph$ derivatives respectively[19,20]).

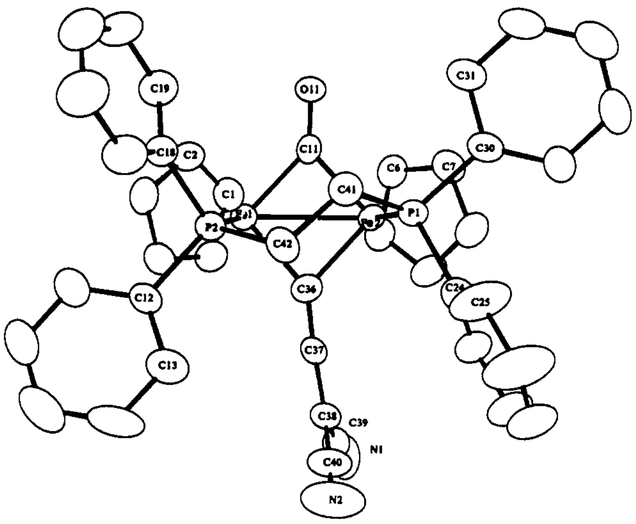

Figure 2. ORTEP plot of complex **3b**.

Crystal Structure of 3b. Results of the X-ray analysis are summarized in Table I and in the Experimental Section. Positional parameters and bond lengths and angles are given in Table IV and V, and a perspective view of the molecule is shown in Figure 2. We will not discuss the overall geometry since it is again typical of such cyclopentadienyldiiron complexes. The μ-3,3-dicyanoallenylidene ligand is almost linear (C36–C37–C38 = 173.8 (5)°), and the dicyanomethylene unit is roughly perpendicular to the Fe_2–μ-C plane (99.3 (7)°) as expected for an allene derivative. The allenylidene ligand is bridging the two iron atoms in the σ, σ (2e) mode. The formal iron–iron bond order is again 1 (Fe1–Fe2 = 2.515 (1) Å). The bridging allenylidene and carbonyl ligands have very close bonding parameters with respect to the diiron core (see Fe–μ-C distances and Fe1–μ-C–Fe2 angles) so that these two ligands have similar σ-donating/π-accepting properties. The C_α–C_β (C36–C37 = 1.258 (5) Å) bond is notably short, indicating a bond order between 2 and 3, the C_β–C_γ being a typical double carbon–carbon bond (C37–C38 = 1.345 (6) Å). Very similar parameters have been observed in the only two other known X-ray structures of μ-allenylidene bimetallic complexes. These complexes are $[W(CO)_5]_2(\mu$-$C{=}C{=}CPh_2)$,[14c] which contains a W–W bond

---

(17) March, J. R. *Advanced Organic Chemistry*, 3rd ed.; Wiley: New York, 1985.

(18) Little, R. G.; Pautler, D.; Coppens, P. *Acta Crystallogr., Sect. B* **1971**, *B27*, 1493.

(19) Kirchner, R. M.; Ibers, J. A. *J. Organomet. Chem.* **1974**, *82*, 243.

(20) Hossain, M. B.; Hanlon, D. J.; Marten, D. F.; Van der Helm, D.; Dehmlow, E. V. *Acta Crystallogr., Sect. B* **1982**, *B38*, 1457.

Table IV. Positional Parameters and Their Estimated Standard Deviations for 3b[a]

atom	*x*	*y*	*z*	*B*, Å^2
Fe1	0.63333 (4)	0.14221 (6)	0.04148 (3)	2.30 (2)
Fe2	0.53949 (3)	0.24457 (6)	0.04205 (3)	2.33 (2)
Cl1	0.2215 (1)	0.7366 (3)	0.5473 (1)	9.67 (8)*
P1	0.53737 (6)	0.2625 (1)	0.12637 (6)	2.47 (3)
P2	0.68333 (7)	0.1266 (1)	0.12540 (6)	2.50 (3)
O11	0.5271 (2)	0.0375 (3)	0.0633 (2)	3.22 (9)
N1	0.6629 (3)	0.5418 (5)	−0.0307 (3)	5.3 (2)
N2	0.7338 (4)	0.5300 (6)	0.1479 (3)	8.0 (2)
C′	0.2224 (6)	0.727 (1)	0.4697 (5)	12.3 (4)*
C1	0.6103 (3)	0.0996 (5)	−0.0407 (3)	3.7 (1)
C2	0.6298 (3)	0.0172 (5)	−0.0086 (2)	3.6 (1)
C3	0.6906 (3)	0.0341 (5)	0.0201 (2)	3.5 (1)
C4	0.7089 (3)	0.1275 (5)	0.0063 (2)	3.5 (1)
C5	0.6594 (3)	0.1672 (5)	−0.0311 (2)	3.4 (1)
C6	0.4749 (3)	0.2060 (5)	−0.0286 (3)	3.5 (1)
C7	0.4438 (3)	0.2436 (5)	0.0089 (3)	3.7 (1)
C8	0.4644 (3)	0.3419 (5)	0.0201 (3)	3.7 (2)
C9	0.5070 (3)	0.3647 (5)	−0.0106 (3)	3.5 (1)
C10	0.5139 (3)	0.2796 (5)	−0.0403 (2)	3.4 (1)
C11	0.5554 (2)	0.1077 (4)	0.0559 (2)	2.4 (1)
C12	0.7651 (3)	0.1623 (5)	0.1382 (2)	2.8 (1)
C13	0.7845 (3)	0.2560 (5)	0.1526 (2)	3.8 (1)
C14	0.8469 (3)	0.2801 (6)	0.1638 (3)	5.4 (2)
C15	0.8903 (3)	0.2126 (7)	0.1581 (3)	5.2 (2)
C16	0.8713 (3)	0.1212 (6)	0.1404 (3)	4.9 (2)
C17	0.8096 (3)	0.0948 (5)	0.1314 (3)	4.1 (2)
C18	0.6889 (3)	0.0048 (5)	0.1562 (2)	2.9 (1)
C19	0.6548 (3)	−0.0728 (5)	0.1301 (3)	3.7 (2)
C20	0.6598 (4)	−0.1648 (5)	0.1529 (3)	5.0 (2)
C21	0.6989 (4)	−0.1799 (6)	0.2025 (3)	5.6 (2)
C22	0.7324 (4)	−0.1040 (6)	0.2284 (3)	5.8 (2)
C23	0.7274 (3)	−0.0126 (5)	0.2062 (3)	4.3 (2)
C24	0.5561 (3)	0.3839 (5)	0.1569 (2)	3.0 (1)
C25	0.5643 (4)	0.3971 (6)	0.2115 (3)	5.6 (2)
C26	0.5768 (5)	0.4898 (6)	0.2328 (3)	7.3 (3)
C27	0.5815 (4)	0.5689 (6)	0.2017 (3)	5.7 (2)
C28	0.5713 (4)	0.5572 (5)	0.1477 (3)	4.8 (2)
C29	0.5597 (3)	0.4642 (5)	0.1256 (3)	3.7 (2)
C30	0.4623 (3)	0.2375 (5)	0.1408 (2)	3.1 (1)
C31	0.4415 (3)	0.1410 (5)	0.1408 (3)	4.4 (2)
C32	0.3842 (3)	0.1225 (6)	0.1513 (3)	5.6 (2)
C33	0.3468 (3)	0.1959 (6)	0.1610 (3)	5.0 (2)
C34	0.3660 (3)	0.2899 (6)	0.1594 (3)	5.2 (2)
C35	0.4235 (3)	0.3115 (5)	0.1497 (3)	4.2 (2)
C36	0.6261 (3)	0.2794 (4)	0.0538 (2)	2.8 (1)
C37	0.6536 (3)	0.3604 (5)	0.0585 (3)	3.2 (1)
C38	0.6782 (3)	0.4504 (5)	0.0591 (3)	3.7 (2)
C39	0.6715 (3)	0.5031 (5)	0.0101 (3)	3.7 (2)
C40	0.7094 (3)	0.4968 (5)	0.1079 (3)	4.7 (2)
C41	0.5888 (3)	0.1823 (5)	0.1745 (2)	3.1 (1)
C42	0.6567 (3)	0.2002 (5)	0.1755 (2)	3.1 (1)

[a] Starred *B* values are for atoms that were refined isotropically. *B* values for anisotropically refined atoms are given in the form of the isotropic equivalent displacement parameter defined as $(4/3)[a^2B(1,1) + b^2B(2,2) + c^2B(3,3) + ab(\cos\gamma)B(1,2) + ac(\cos\beta)B(1,3) + bc(\cos\alpha)B(2,3)]$.

and no additional bridging ligand (C_α–C_β = 1.28 (4) Å, C_β–C_γ = 1.32 (4) Å), and $[Mn(CO)_4]_2(\mu\text{-}CO)(\mu\text{-}C{=}C{=}C^tBu_2)$,[14e] which contains a Mn–Mn bond and a bridging carbonyl ligand (C_α–C_β = 1.27 (2) Å, C_β–C_γ = 1.39 (2) Å). In allene, the carbon–carbon bond length is 1.31 Å.[17] Hence, whatever the complex (different metal, substituents, etc), the C_α–C_β bond is always shortened and C_β–C_γ is always elongated. We may then propose that this results intrinsically from the interaction of an allenylidene ligand with a bimetallic framework, i.e., the phenomenon would be orbital in nature.

Table V. Selected Bond Lengths (Å) and Angles (deg) with Esd's for 3b[a]

	Bond Lengths		
Fe1–Fe2	2.515 (1)	Fe2–Ct″	1.741 (1)
Fe1–P2	2.198 (2)	C36–C37	1.258 (5)
Fe1–C11	1.913 (6)	C37–C38	1.345 (6)
Fe1–C36	1.916 (6)	C38–C39	1.431 (6)
Fe1–Ct′	1.747 (1)	C38–C40	1.435 (7)
Fe2–P1	2.196 (2)	O11–C11	1.186 (4)
Fe2–C11	1.922 (6)	N1–C39	1.151 (6)
Fe2–C36	1.937 (6)	N2–C40	1.139 (6)
	Bond Angles		
Fe2–Fe1–P2	106.18 (6)	P1–Fe2–C11	88.3 (2)
Fe2–Fe1–C11	49.2 (2)	P1–Fe2–C36	93.9 (2)
Fe2–Fe1–C36	49.6 (2)	P1–Fe2–Ct″	122.74 (6)
Fe2–Fe1–Ct′	131.61 (4)	C11–Fe2–C36	94.5 (2)
P2–Fe1–C11	93.4 (2)	C11–Fe2–Ct″	122.8 (2)
P2–Fe1–C36	88.6 (2)	C36–Fe2–Ct″	125.2 (2)
P2–Fe1–Ct′	122.21 (6)	Fe1–C11–Fe2	81.9 (2)
C11–Fe1–C36	95.4 (3)	Fe1–C36–Fe2	81.5 (2)
C11–Fe1–Ct′	121.9 (2)	C36–C37–C38	173.8 (5)
C36–Fe1–Ct′	126.2 (2)	C37–C38–C39	119.4 (4)
Fe1–Fe2–P1	106.03 (5)	C37–C38–C40	121.8 (4)
Fe1–Fe2–C11	48.9 (2)	C39–C38–C40	118.7 (4)
Fe1–Fe2–C36	48.9 (2)	N1–C39–C38	175.6 (5)
Fe1–Fe2–Ct″	130.97 (5)	N2–C40–C38	177.0 (6)

[a] Ct^x is the centroid of Cp bonded to Fe*x*.

Variable-Temperature NMR Study. The cyclopentadienyl ligands in cis isomers of monosubstituted (*μ*-alkenylidene)diiron complexes are magnetically inequivalent. Since *cis*-(*μ*-3,4,4-tricyanobuta-1,3-dienylidene)diiron complexes **2a,b** exhibit at room temperature a single resonance in their ^{1}H NMR spectra, we have undertaken variable-temperature experiments in order to understand the reason for this equivalence. In the case of **2b** the experiment was also conducted with the ^{31}P nucleus.

At 298 K in acetone-d_6 (99.6 MHz) complex **2a** exhibits a sharp resonance at δ 8.99 for the H_β proton and a broader ($\nu_{1/2} \sim$ 6 Hz) single resonance at δ 5.34 for the cyclopentadienyl hydrogens. At 320 K, both resonances are sharp. Cooling the solution below room temperature allows two cyclopentadienyl resonances in a 1/1 ratio to be observed, whereas the H_β resonance remains unchanged. The energy barrier for this dynamic process is not determined with good accuracy, since the spacing between the two cyclopentadienyl signals in the slow-exchange regime is only $\Delta\nu$ = 2 Hz, measured at 99.6 MHz. Using the equation[21]

$$\Delta G^{\ddagger} = 19.14T_c(9.97 + \log T_c/\Delta\nu)\ (\mathrm{J\ mol^{-1}})$$

where T_c is the coalescence temperature, one gets $\Delta G^{\ddagger}_{298}$ = 16 kcal mol^{-1}, with an accuracy not better than 1 kcal mol^{-1}.

The case of **2b** is much more favorable. At room temperature in dichloromethane-d_2 at 300 MHz (^{1}H NMR), a single sharp resonance at δ 4.60 is observed for the cyclopentadienyl protons, and H_β gives a triplet at δ 9.34 (J_{PH} = 2.0 Hz). Upon cooling, the cyclopentadienyl signal starts to broaden. It is again noteworthy that the H_β does not experience any comparable change. The triplet pattern is lost, but the total line width of the signal does not change during the whole experiment. Particularly, at the coalescence temperature of the cyclopentadienyl signals, the H_β signal remains sharp. At the slow-exchange limit ($T \sim$ 190 K), two signals for the cyclopentadienyl protons in a 1/1 ratio are observed with a spacing of $\Delta\nu$ = 86.5 Hz. The corrected coalescence temperature is T_c = 211 K. Hence, the energy barrier for this process is $\Delta G^{\ddagger}_{211}$ = 10.0 ± 0.2 kcal mol^{-1}. The same process, when observed by $^{31}P\{^1H\}$ NMR (121 MHz), leads to the splitting of the room-temperature resonance (δ 61.8) in two equally pop-

---

[21] Günther, H. *NMR Spectroscopy: An Introduction*; Wiley: Chichester, England, 1980.

ulated sites separated by $\Delta\nu$ = 212 Hz. The coalescence temperature of T_c = 213 K leads to $\Delta G^{\ddagger}_{213}$ = 9.7 ± 0.2 kcal mol^{-1}, in accordance with the ^{1}H NMR data.

The best way to fit the data is to invoke a more or less restricted rotation of the tricyanobutadienylidene ligand about the bridging carbon C_α–C_β bond. The 6 kcal mol^{-1} energy difference between complexes **2a** and **2b** for this process accounts for the importance of the dipolar mesomeric form (Scheme I): the more electron rich the diiron moiety, the more stabilized the dipolar form, the lower the barrier to rotation. Similar behavior[22] has been observed for (vinylcarbyne)diiron cations of the type $\{[CpFe(CO)](\mu\text{-}CO)(\mu\text{-}CCH{=}CHR)]\}^+$. The highest rotational barrier about the C_α–C_β bond, observed for a strong electron-releasing group R = $N(CH_3)_2$, is $\Delta G^{\ddagger}$ = 19.8 (1) kcal mol^{-1}. From the X-ray structure,[23] the complex exhibits bond lengths of 1.377 (10) Å for the C_α–C_β bond and 1.391 (1) and 1.295 (9) Å for respectively the C_β–C_γ and C_γ–N bonds. These data are to be compared to those for **2a**: $\Delta G^{\ddagger}_{298}$ = 16 ± 1 kcal/mol^{-1}, C_α–C_β = 1.358 (5) Å, C_β–C_γ = 1.406 (5) Å, and C_γ–C_δ = 1.382 (5) Å. The authors carried out Fenske–Hall molecular orbital calculations on their complexes.[22] It was shown that, during rotation, conjugation between the μ-vinyl unit and the diiron-bridging carbon moiety was not destroyed. As already mentioned, others have conducted the same type of calculations on μ-ethenylidene complex **1a**.[4] The C_α–C_β π-bond of μ-ethenylidene, perpendicular to the Fe–C_α–C_β–Fe plane, scarcely interacts with the diiron framework. Qualitatively, attachment of a strongly electron-withdrawing group such as the tricyanovinyl group will remove electron density from this orbital, allowing rotation. The remaining orbital interactions are then similar in the two systems.[4,22] Hence, by choosing the substituents on the bridging ligands, we propose that a continuum can be drawn between electron-rich μ-vinylcarbyne ligands and highly electron-deficient μ-butadienylidene ligands.

Electronic Absorption Spectra. This study was undertaken because we were puzzled by the high intensity and the color of the μ-3,4,4-tricyanobuta-1,3-dienylidene complexes **2a** (golden red) and **2b** (violet). As a reference we have recorded the spectra of the parent μ-ethenylidene complexes **1a** (red-purple) and **1b** (green). The electronic absorption spectra were recorded between 300 and 800 nm, in dichloromethane at room temperature.

The spectrum of $[CpFe(CO)]_2(\mu\text{-}CO)(\mu\text{-}C{=}CH_2)$ exhibits the following features [λ_{max}, nm (ϵ, L mol^{-1} cm^{-1})]: 530 (1100), 415 (sh, 1400), 330 (7200). This spectrum is very similar to those of $[CpFe(CO)_2]_2$[24] and $[CpFe(CO)]_2(\mu\text{-}CO)(\mu\text{-}CHCH_3)$,[25] which is not surprising since the ethenylidene, carbonyl, and alkylidene fragments have similar bonding interactions with the diiron fragment, again keeping in mind that the occupied π-system of the ethenylidene is not involved in the bonding.[4] Hence, we will follow previous assignments[24,25] that the UV band at 330 nm is due to the $\sigma \rightarrow \sigma^*$ transition. Similarly, the weaker absorptions at 530 and 415 nm are assigned to $d\pi \rightarrow \sigma^*$ transitions.

More interesting is the spectrum of the μ-tricyanobutadienylidene complex **2a** (Figure 3). The main additional feature is the strong absorption (ϵ = 25 500 L mol^{-1} cm^{-1}) centered at 476 nm, the $\sigma \rightarrow \sigma^*$ band remaining essentially unchanged at 332 nm. This absorption is then a direct consequence of the tricyanovinyl substitution of the ethenylidene ligand. Such an allowed transition may

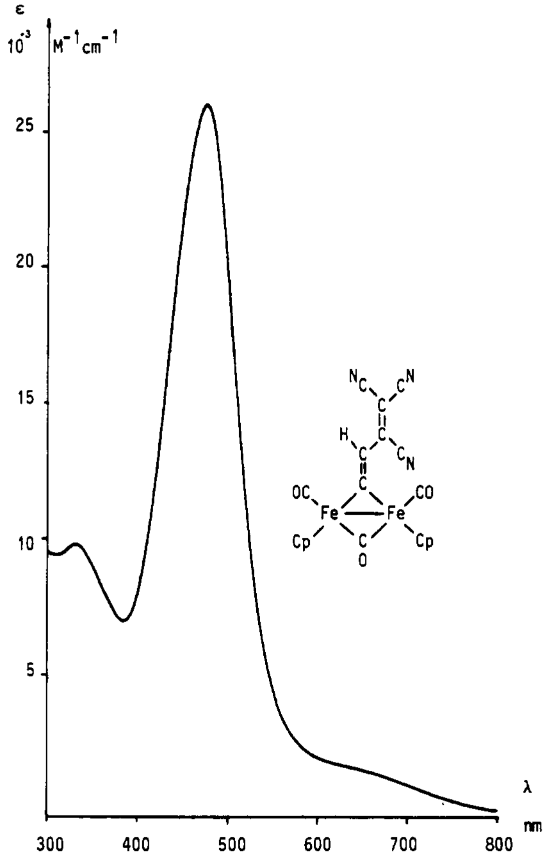

Figure 3. Electronic absorption spectra of complex **2a**.

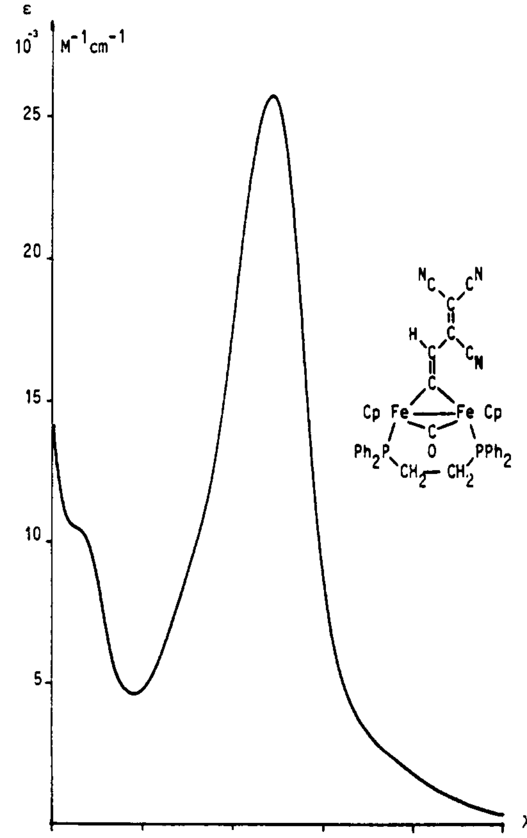

Figure 4. Electronic absorption spectra of complex **2b**.

---

(22) Casey, C. P.; Konings, M. S.; Marder, S. R.; Takezawa, Y. *J. Organomet. Chem.* **1988**, *358*, 347.

(23) Casey, C. P.; Konings, M. S.; Marder, S. R. *Polyhedron* **1988**, *7*, 881.

(24) Abrahamson, H. B.; Palazotto, M. C.; Reichel, C. L.; Wrighton, M. S. *J. Am. Chem. Soc.* **1979**, *101*, 4123.

(25) McKee, S. D.; Bursten, B. E. *J. Am. Chem. Soc.* **1991**, *113*, 1210.

Table VI. Cyclic Voltammetry Data[a]

complex	$E_{1/2}^{ox1}$, V	ΔE_p, mV	$E_{1/2}^{red1}$, V	ΔE_p, mV
$[CpFe(CO)_2]_2$	0.20	80	−2.08 (−2.01)[b]	
1a	0.25[c]	100	−2.13	80
1b	−0.50	70		
2b	0	0	−1.72	80
2c	0.05	80	−1.70	80
3b	0	70	−1.89	80

[a] CH_2Cl_2–Bu_4NPF_6 electrolyte; vitreous carbon electrode; scan rate 0.2 V/s unless stated otherwise. [b] Irreversible 2e process: E_p ($E_{p/2}$). [c] Scan rate 0.5 V/s.

arise from either a MLCT or a ligand based $\pi \rightarrow \pi^*$. The problem of the assignment is first addressed by looking at the spectrum of the dppe congener **2b** (Figure 4). Again the most striking feature of the spectrum is the strong absorption (ϵ = 25 700 L mol^{-1} cm^{-1}) now centered at 539 nm, the compound being violet. Hence, substitution of dppe for carbonyls leads to a bathochromic shift of the absorption, the shape and intensity of the bands ensuring that they arise from the same type of transition. If this transition was a dimetal to bridging ligand charge transfer (MLCT), a pronounced solvent dependence would be expected.[26] In acetone or methylmethacrylate the absorption is observed at 546 nm, and taking into account the width of the band, the shift is almost negligible. Consequently, we propose that the strong band observed in the electronic spectra of complexes **2a,b** is largely ligand $\pi \rightarrow \pi^*$ based. This is quite interesting since by carefully choosing the substituents on the iron atoms there is an actual way of tuning the absorption and thereby the dyeing properties of our complexes. This is reminiscent of the use of organic dyes obtained by association of tricyanovinyl, tricyanobutadienyl, and related groups with electron-rich moieties allowing good conjugation such as substituted phenyls and heterocycles.[7] It is also noteworthy that (μ-alkenylidene)diplatinum complexes[27] and, more recently, related cyanine-substituted bis(diiron) systems[28] have been shown to have unusual, intriguing photochemical and photophysical properties.

Electrochemistry. The electrochemical behavior of the μ-ethenylidene, μ-buta-1,3-dienylidene, and μ-allenylidene complexes has been investigated by cyclic voltammetry in order to assess the effects of (i) modifying the bridging alkenylidene ligand and (ii) substituting dppe for CO on the primary redox potentials of the complexes. This should provide an insight into the mechanism of the μ-buta-1,3-dienylidene complex **2**-forming reaction in that it will make possible to check on the feasibility of a homogeneous redox reaction between **1a** or **1b** and tcne (see below, mechanism of the reaction). The primary redox potentials of the complexes are listed in Table VI along with those of the parent $[CpFe(CO)_2]_2$. Apart from the reduction of $[CpFe(CO)_2]_2$, all the primary steps involve one electron as indicated by the anodic-to-cathodic peak separation (ΔE_p,[29,30] Table VI), close to that measured for ferrocene (ΔE_p = 60–70 mV) under similar conditions. The secondary oxidation and/or reduction steps will not be discussed here, except for complexes **2b–c**.

Substitution of C=CH$_2$ for CO in a bridging position does not result in pronounced changes of the primary reduction or oxidation potentials (Table VI). However, the kinetic stability of the products of these electron-transfer steps is reversed on going from the unsubstituted complex to the bridging vinylidene **1a**: whereas the oxidation of $[CpFe(CO)_2]_2$ is chemically almost reversible in the CH_2Cl_2–Bu_4NPF_6 electrolyte at a scan rate of 0.2 V/s (i_p^c/i_p^a = 0.73 at 0.05 V/s and 0.95 at 0.2 V/s),[30,31] that of **1a** appears much less so (i_p^c/i_p^a = 0.50 at 0.5 V/s). On the contrary, the alkenylidene complex presents a fully reversible reduction on the cyclic voltammetry time scale, while $[CpFe(CO)_2]_2$ is cleaved on 2e reduction. The substitution of the electron-releasing dppe for the terminal CO groups leads, as expected, to a large negative shift of both primary redox potentials: **1b** does not reduce in the potential domain available in the electrolyte–solvent system whereas its oxidation ($E_{1/2}$ = 0.50 V) is by 0.75 V easier than that of its precursor **1a**. The presence of the bridging diphosphine also results in a strong stabilization of the radical cation since the oxidation of **1b** is a fully reversible process (i_p^c/i_p^a = 1; ΔE_p = 70 mV) on the time scale of the CV experiment (0.04 V/s < v < 1 V/s). A similar clamping effect of the bridging diphosphine has been observed in the case of the $[CpFe(\mu\text{-}CO)]_2(\mu\text{-dppe})$ analogue of **1b**.[32]

The introduction of the electron-withdrawing tricyanovinyl group results in a positive shift of the oxidation potential of **2b** with respect to that of **1b** ($\Delta E_{1/2}^{ox}$ = 0.5 V). From the data in Table VI, it appears that dppm and dppe have similar electonic effects since the redox potentials of **2b** and **2c** are only marginally different. However, the nature of the bridging diphosphine affects the second oxidation process of the complexes; the second oxidation of **2c** ($E_{1/2}^{ox2}$ = 0.68 V) appears as chemically reversible ($(i_p^c/i_p^a)^{ox2}$ = ca. 1) but electrochemically quasi-reversible with a large peak separation (ΔE_p^{ox2} = 180 mV). Repetitive CV's on this process confirm the chemical reversibility since the peak currents are conserved and no other peak is detected. This suggests that a reversible structural rearrangement,[33] which does not lead to disruption of the complex, is coupled to the oxidation of **2c**$^{\bullet +}$. Similarly, a second oxidation with an apparent $E_{1/2}^{ox2}$ = 0.66 V, and which displays the characteristics of a pseudoreversible couple (ΔE_p^{ox2} = 180 mV) is observed for **2b**. However, a close inspection of the second oxidation of **2b** shows that, for this species, two different radical cations and two different dications do exist and interconvert on the CV time scale (Figure 5). Whereas Figure 5a illustrates the reversibility of the primary oxidation (and reduction) process, the *ramp–clamp*[35] CV's in Figures 5b–d demonstrate the occurrence of chemical steps coupled to the electron transfers: the presence of a reversible couple with $E_{1/2}$ = 0.59 V, due to the reduction of the rearranged dication **2b**$_R^{2+}$ (the subscripts I and R stand respectively for

---

(26) See for example: Ratliff, K. S.; DeLaet, D. L.; Gao, J.; Fanwick, P. E.; Kubiak, C. P. *Inorg. Chem.* **1990**, *29*, 4022.

(27) Baralt, E.; Boudreaux, E. A.; Demas, J. N.; Lenhert, P. G.; Lukehart, C. M.; McPhail, A. T.; McPhail, D. R.; Myers, J. B.; Sacksteder, L.; True, W. R. *Organometallics* **1989**, *8*, 2417.

(28) Spotts, J. M.; Schaefer, W. P.; Marder, S. R. *Abstracts of Papers*, Fourth Chemical Congress of North America, New York, Aug 1991; American Chemical Society: Washington, DC, 1991; INOR 335.

(29) The abbreviations used in this paper are as follows: CV, cyclic voltammetry; i_p^a and i_p^c, anodic and cathodic peak currents; ΔE_p, anodic-to-cathodic peak separation; v, scan rate.

(30) Bard, A. J.; Faulkner, L. R. *Electrochemical Methods. Fundamentals and Applications*; John Wiley: New York, 1980; pp 228–9.

(31) This result is in contrast with a previous report by Meyer and co-worker,[31a] but in fair agreement with those of Legzdins et al.[31b] and Mann et al.[31c] (a) Ferguson, J. A.; Meyer, T. J. *Inorg. Chem.* **1971**, *10*, 1025. (b) Legzdins, P.; Wassink, B. *Organometallics* **1984**, *3*, 1811. (c) Bullock, J. P.; Palazotto, M. C.; Mann, K. R. *Inorg. Chem.* **1991**, *30*, 1284.

(32) Ferguson, J. A.; Meyer, T. J. *Inorg. Chem.* **1972**, *11*, 631.

(33) For a review on structural rearrangements coupled with electron-transfer steps, see: Geiger, W.E. *Prog. Inorg. Chem.* **1985**, *33*, 275. Evans, D. H.; O'Connell, K. M. *Electroanal. Chem.* **1986**, *14*, 113.

(34) Al-Salih, T. I.; Pickett, C. J.; Richards, R. L.; Talarmin, J.; Pombeiro, A. J. L. *Port. Electrocheim. Acta* **1985**, *3*, 35. Al-Salih, T. I.; Pickett, C. J. *J. Chem. Soc., Dalton Trans.* **1985**, 1255.

(35) Froom, S. F. T.; Green, M.; Nagle, K. R.; Williams, D. J. *J. Chem. Soc., Chem. Commun.* **1987**, 1305.

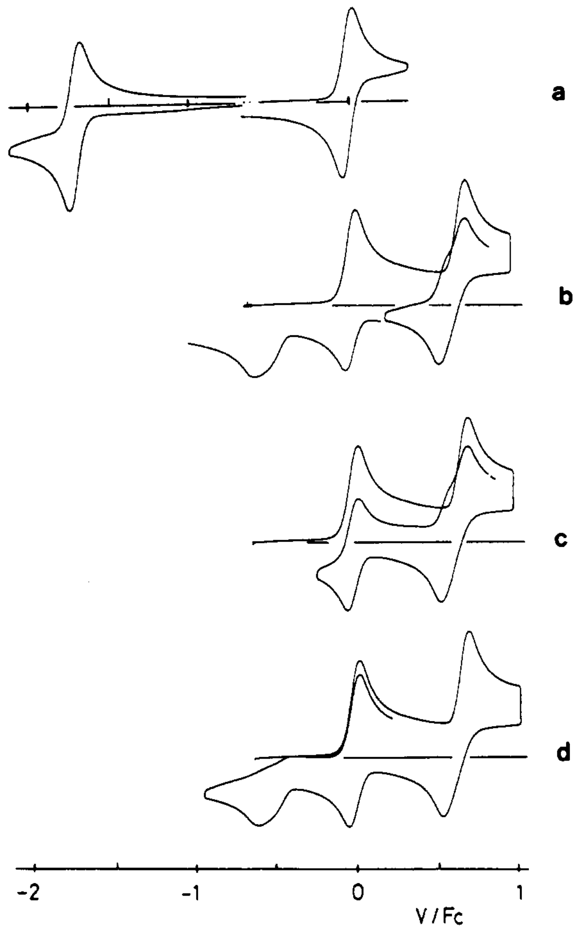

Figure 5. (a) Cyclic voltammetry of **2b** showing reversibility of the primary redox processes and ramp–clamp cyclic voltammetry (10 s hold at the upper limit) showing (b) the presence of the $\mathbf{2b_R}^{\bullet+}/\mathbf{2b_R}^{2+}$ couple and the reduction of $\mathbf{2b_R}^{\bullet+}$ and (c–d) the influence of the switching potential on the regeneration of $\mathbf{2b_I}$.

the initial and rearranged geometry of 2) to $\mathbf{2b_R}^{\bullet+}$, is shown in Figure 5b as well as a new reduction peak (E_p^{red} = –0.63 V). This process is assigned to the reduction of $\mathbf{2b_R}^{\bullet+}$ to $\mathbf{2b_I}$ on the basis of the experiments illustrated in Figure 5c–d: the oxidation peak of $\mathbf{2b_I}$ is smaller on the second anodic scan than on the initial one, when the potential scan is reversed before the irreversible reduction at –0.63 V has been traversed (Figure 5c); this demonstrates that some material with the initial geometry has been lost as a result of the second oxidation of the complex. On the contrary, Figure 5d shows that the starting material $\mathbf{2b_I}$ is almost completely regenerated when the irreversible reduction is included in the potential domain before scan reversal. Repetitive CV's on the second oxidation demonstrate that the peak due to the oxidation of $\mathbf{2b_I}^{\bullet+}$ is not completely suppressed and, therefore, that this species is partly regenerated from $\mathbf{2b_R}^{\bullet+}$. These reactions are summarized in Scheme II. The main difference between **2b** and **2c**, as far as the structural rearrangement is concerned, lies in the different stabilities of the $\mathbf{2_I}^{2+}$ and $\mathbf{2_R}^{\bullet+}$ species which are both less labile for the dppe complex than for its dppm counterpart. The nature of the observed structural rearrangement and the role of the bridging diphosphine in this process are unclear.

Protonation of the μ-Allenylidene Complex 3b. The reactivity of μ-allenylidene complexes is almost unexplored.[15] Actually, only in the case of (μ-σ,η^2-(4e)-allenylidene)dimolybdenum and -ditungsten derivatives has such a problem been addressed. Nucleophiles (H^-) attack at C_γ, whereas protonation occurs at C_α.[35]

Scheme II

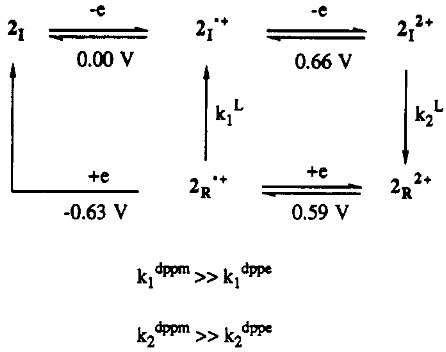

Treatment of the (μ-dicyanoallenylidene)iron complex **3b** with $HBF_4 \cdot OMe_2$ at 0 °C in dichloromethane (eq 3) results after workup in the isolation of crystals of the cationic (μ-(2,2-dicyanovinyl)carbyne)diiron complex $Cp_2Fe_2(\mu\text{-}CO)(\mu\text{-dppe})[\mu\text{-}CCH{=}C(CN)_2]^+BF_4^-$ (**4b**). A weak nitrile band is observed at 2220 cm^{-1} in the infrared spectrum (dichloromethane) of the complex whereas the bridging carbonyl gives an absorption at 1785 cm^{-1}. In the ^1H NMR spectrum (acetone-d_6, room temperature), H_β appears at δ 9.30 as a triplet due to coupling with the phosphorus atoms (J_{HP} = 1.9 Hz). Also good evidence for a μ-vinylcarbyne formulation[23] comes from the ^{13}C NMR spectrum. The bridging carbon C_α is shifted downfield at δ 417.0. Again a triplet pattern is observed due to the coupling with the phosphorus atoms (J_{PC} = 15 Hz). The C_β carbon gives a doublet at δ 190.3 with a 157-Hz coupling with the attached proton. The C_γ carbon bearing the two nitrile groups is observed at high field (δ 63.0).

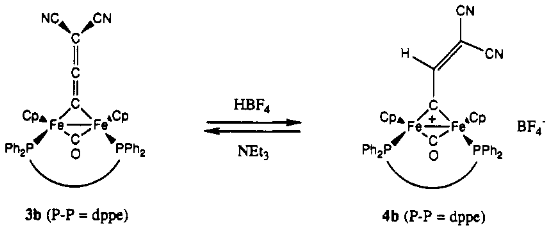

(3)

Thus, protonation of a symmetrically bridged (μ-σ,σ-(2e)-allenylidene)diiron complex, yielding a μ-vinylcarbyne complex, occurs at C_β just as in the case of μ-alkenylidene complexes.[15] A mononuclear cationic (vinylcarbyne)manganese complex $[CpMn(CO)_2{\equiv}CCH{=}CPh_2]^+$ has been obtained[36] by protonation of the allenylidene precursor $CpMn(CO)_2{=}C{=}C{=}CPh_2$, and we have already mentioned that protonation occurs at C_α in the case of (μ-σ,η^2-(4e)-allenylidene)dimolybdenum and -ditungsten complexes.[35]

We also found that the protonation was entirely reversible, addition of an excess of triethylamine to a solution of **4b** giving back complex **3b** in 100% spectroscopic yield (eq 3). As far as we are aware, deprotonation of a cationic (μ-vinylcarbyne)diiron complex has been reported only once,[37] whereas nucleophiles have been shown to add at the remote vinyl carbon C_γ.[38] Deprotonation of a cationic (μ-pent-2-enylidyne)diiron complex leads to a μ-penta-1,3-dienylidene complex by deprotonation at the C_δ carbon (Scheme III). Hence the H_δ proton in cationic μ-vinyl-

---

[36] Kolobova, N. E.; Ivanov, L. L.; Zhvanko, O. S.; Khitrova, O. M.; Batsanov, A. S.; Struchkov, Y. T. *J. Organomet. Chem.* **1982**, *262*, 39.

[37] Casey, C. P.; Marder, S. R. *Organometallics* **1985**, *4*, 411.

[38] Casey, C. P.; Konings, M. S.; Marder, S. R. *J. Organomet. Chem.* **1988**, *345*, 125.

Scheme III

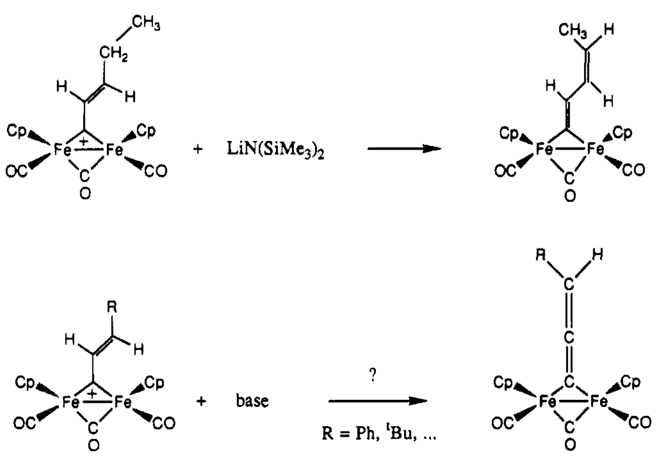

Scheme IV

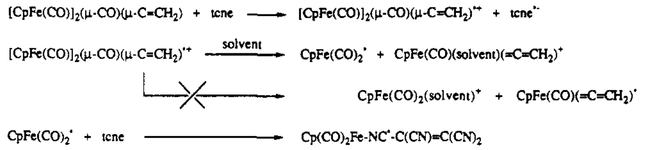

$$[CpFe(CO)]_2(\mu\text{-}CO)(\mu\text{-}C{=}CH_2) + tcne \longrightarrow [CpFe(CO)]_2(\mu\text{-}CO)(\mu\text{-}C{=}CH_2)^{\bullet+} + tcne^{\bullet-}$$

$$[CpFe(CO)]_2(\mu\text{-}CO)(\mu\text{-}C{=}CH_2)^{\bullet+} \xrightarrow{\text{solvent}} CpFe(CO)_2^{\bullet} + CpFe(CO)(solvent)({=}C{=}CH_2)^{+}$$

$$\not\longrightarrow CpFe(CO)_2(solvent)^{+} + CpFe(CO)({=}C{=}CH_2)^{\bullet}$$

$$CpFe(CO)_2^{\bullet} + tcne \longrightarrow Cp(CO)_2Fe\text{-}NC^{\bullet}\text{-}C(CN){=}C(CN)_2$$

carbyne complexes, when present, appears to be more acidic than the H_β ones (the H_δ protons are pseudo-allylic). Consequently, taking into account the deprotonation of our μ-(2,2-dicyanovinyl)carbyne complex that bears no other protons than H_β, it can be proposed that new (μ-allenylidene)diiron complexes could in principle be prepared via the cationic μ-vinylcarbyne deprotonation sequence in the cases where the remote vinyl substituents bear no reactive acidic hydrogens such as phenyl, *tert*-butyl, etc. groups (Scheme III).

Mechanism of the Reaction between μ-Alkenylidene Complexes and tcne. The reaction between μ-ethenylidene complexes **1a** or **1b** and tcne was studied by both ESR and ^{1}H NMR techniques. Although detailed kinetic analyses were not carried out, reliable data are presented that allow a mechanism of these reactions to be discussed.

ESR Spectra. We had previously observed[8] that the reaction between **1a** and tcne produced two types of radical species observable by ESR at room temperature indicating that a single electron transfer between the two reactants was operative. These radicals are the radical anion tcne$^{\bullet-}$ and a mononuclear iron imino tricyanoallyl radical $CpFe(CO)_2N{=}C^{\bullet}C(CN){=}C(CN)_2$ formed through the sequence outlined in Scheme IV. This oxidative iron–iron bond cleavage mechanism has been disclosed previously[39] during the reaction of $[CpFe(CO)_2]_2$ with tcne, a reaction that ultimately leads to $CpFe(CO)_2(CN)$.[40] When we consider the electrochemical data, it is obvious that, if an electron transfer occurs between **1a** (E_p = 0.25 V) and tcne ($E_{1/2}$ = −0.17 V), it is not thermodynamically favored and would have to take place through a charge-transfer complex.[41] Furthermore, a mechanism leading to re-formation of a bimetallic complex could not be satisfyingly written. When we turned to the reaction between the diphosphine-bridged complex **1b** and tcne, where the electrochemical data indicate a favorable single electron transfer ($E_{1/2}(\mathbf{1b}^+/\mathbf{1b})$ = −0.50 V), only the radical anion tcne$^{\bullet-}$ was observed at room temperature,[9] ensuring that the electron transfer did not lead to iron–iron bond breaking in this case.

^{1}H NMR Studies. In order to gain more information, we also studied the course of the reactions by ^{1}H NMR. We were surprised to record well-resolved spectra.

In the case of the diphosphine-bridged complex **1b** and tcne in $CDCl_3$ at room temperature no intermediates are observed. The reaction is virtually complete within 30 min. The only iron-containing species were complexes **2b** and **3b** in ca. 5/1 ratio. Also observed is a signal at δ 3.6 attributed to malononitrile, by comparison to the spectrum of an authentic sample.

The reaction between complex **1a** and tcne is more complex. A typical run in dichloromethane-d_2 (99.6 MHz, [**1a**] = [tcne] ~ 7.5 10^{-2} M) is described herein. Complex **1a** exhibits for the cis isomer a cyclopentadienyl proton signal at δ 4.74, and the methylene protons give a signal at δ 6.89; for the trans isomer these signals appear respectively at δ 4.78 and 6.81.

At a reaction time of 7 min, the spectrum mainly shows the appearance of an intermediate A characterized by two set of signals whose chemical shifts and integral values indicate that species A is a dinuclear complex with a structure reminiscent of that of **1a**. One isomer has a cyclopentadienyl proton signal at δ 4.85 and a methylene signal at δ 7.21 (ratio 5/1), and the other isomer has signals at respectively δ 4.90 and 7.09 (ratio 5/1). Thus species A is a dinuclear complex with cis and trans isomers arising from the interaction of μ-ethenylidene complex **1a** and tcne: it is worth noting that this interaction does not modify the electronic distribution to a large extent. Particularly, the comparison between the methylene chemical shifts of A to those of **1a** ensures that no change in the hybridization occurs so that it remains sp^2. On this basis, a dipolar formulation can be rejected. The following spectra clearly show that species A is quite stable, that its concentration increases during the first 30 min of the reaction, and that it is actually an *intermediate* leading from **1a** to **2a**. Despite these data, we have not been able to further clarify the identity of intermediate A.[42] The signal at δ 5.02 is attributed to the cyclopentadienyl protons of **2a**. It is also obvious that other species are formed especially if one considers the broad cyclopentadienyl resonances around δ 5.0 and the signals below δ 4.0, but the reaction remains relatively clean. The sharp signal at δ 3.6 is again attributed to malononitrile indicating that the μ-allenylidene complex $[CpFe(CO)]_2(\mu\text{-}CO)[\mu\text{-}C{=}C{=}C(CN)_2]$ analogous to **3b** is formed, but we did not succeed to isolate it.[43] It is also to be noted that cis and trans isomers of complex **2a** are formed, the H_β proton signals being at δ 9.00 and 8.80. Upon crystallization only the cis isomer is isolated (see above).

---

[39] Krusic, P. J.; Stoklosa, H.; Manzer, L. E.; Meakin, P. J. *J. Am. Chem. Soc.* **1975**, *97*, 667.

[40] Su, S. R.; Wojcicki, A. *Inorg. Chem.* **1975**, *14*, 89.

[41] (a) Kaim, W. *Acc. Chem. Res.* **1985**, *18*, 160. (b) Kochi, J. K. *Organometallic Mechanisms and Catalysis*; Academic Press: New York, 1978.

[42] We have initially proposed a charge-transfer complex between **1a** and tcne for species A. Its relatively high concentration and its formation over 30 min argue against this formulation as suggested by a reviewer. Although attractive, the data indicate that A cannot be the tetracyanoalkyl-substituted alkenylidene $[CpFe(CO)]_2(\mu\text{-}CO)[\mu\text{-}C{=}CHC(CN)_2C(CN)_2H]$, since, by integration, a methylene and not a methine signal is observed. The initially sought [2 + 2] cycloadduct $[CpFe(CO)]_2(\mu\text{-}CO)[\mu\text{-}CCH_2C(CN)_2C(CN)_2]$ would give an AB type spectrum for the methylene signal in the cis isomer and, therefore, is not species A. The fact that the charges are not yet separated in A suggest it may precede, along the reaction coordinate, a dipolar structure. Attempts to isolate A at early stages of the reaction have failed.

[43] In $^{13}C\{^1H\}$ NMR spectra of crude reaction mixtures between **1a** and tcne, we have observed signals at δ 206, 171, and 45 that could be attributed to $[CpFe(CO)]_2(\mu\text{-}CO)[\mu\text{-}C{=}C{=}C(CN)_2]$.

Scheme V

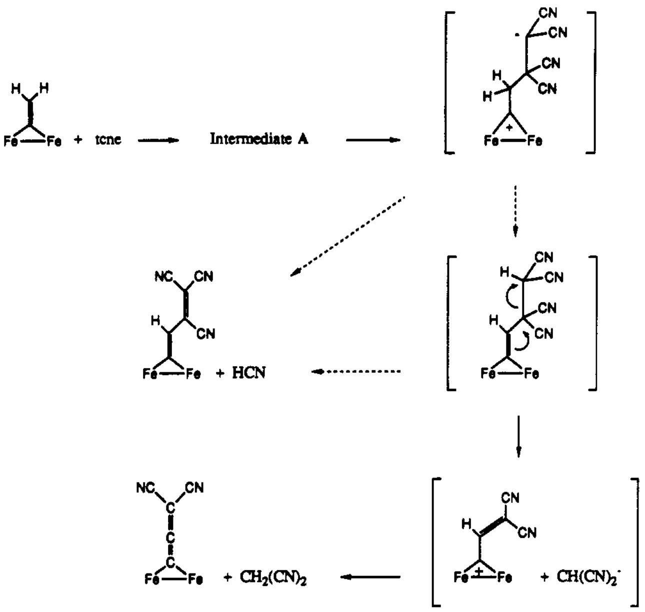

The reaction is complete within 2.5 h in dichloromethane-d_2, but when carried out in acetonitrile-d_3, it requires less than 35 min and about 24 h in benzene-d_6. The increased rate of the reaction with increased solvent polarity may be explained by the obtention of strongly polarized complexes. Hence, we propose that in the first step (apart from the competing electron-transfer sequence; see above), species A is formed as a true intermediate (Scheme V). The following reactions occur with no other observed intermediate. Through effective carbon–carbon bond formation between the electron-rich C_β carbon and electrophilic tcne,[42] intermediate A may then give the zwitterion whose fate depends on the H_β hydrogen reactivity. Loss of hydrogen cyanide leads to μ-tricyanobutadienylidene complexes. Another pathway is available through [1,3] proton migration, leading to an unstable tetracyanoalkyl-substituted μ-alkenylidene complex (loss of HCN might occur at this stage as well). Carbon–carbon bond cleavage produces a μ-(dicyanovinyl)carbyne complex and the malononitrile anion, and further deprotonation yields μ-allenylidene complexes and malononitrile. In support of this scheme, we have shown that the cationic μ-vinylcarbyne complex **3b** was deprotonated by triethylamine ($pk_a \sim 11$);[17] the malononitrile anion has a comparable basicity ($pk_a = 11.2$).[7] The μ-allenylidene formation is then a retro-Michael reaction.

Closely related reactions between electron-rich olefins and tcne have been described and thoroughly studied.[7] Several products including charge-transfer complexes, tetracyanoalkyl compounds, [2 + 2] cycloadducts, zwitterions, and tricyanovinylation compounds have been characterized. Very often, the tricyanovinylation compounds are thermodynamically favored and Michael-type or [2 + 2] cycloadducts are intermediates, more or less stable depending on reaction conditions.

Conclusions

In this paper, we have summarized our knowledge of the reaction between (μ-ethenylidene)diiron complexes and tcne. We have shown that the reactivity of the β-hydrogens of the former μ-ethenylidene ligand was the main obstacle to an initially desired μ-cyclobutylidene complex. The isolated polycyano-substituted (μ-butadienylidene)- and (μ-allenylidene)diiron complexes exhibit exciting physicochemical behavior. Further developments, particularly in the fields of optical and electron-transfer properties, are to be expected.

Experimental Section

All reactions were performed under a nitrogen atmosphere with use of standard Schlenk techniques. Toluene and diethyl ether were obtained from purple sodium benzophenone solutions. Dichloromethane and hexanes were dried by refluxing over CaH_2, and acetone was dried by refluxing over B_2O_3. Deuterated solvents were dried over molecular sieves. All solvents were degassed before use. Infrared spectra were recorded on a Perkin-Elmer 1430 spectrophotometer. NMR spectra were recorded on a JEOL FX 100 spectrometer (99.60 MHz for ^1H; 25.05 MHz for ^{13}C; 40.32 MHz for ^{31}P) or on a Bruker AC 300 spectrometer (300.12 MHz for ^1H; 75.47 MHz for ^{13}C; 121.5 MHz for ^{31}P). Electronic spectra were obtained on a Varian Cary 219 UV–vis spectrophotometer in 1-mm-path quartz cells. Analytical data were collected at the Service Central d'Analyse du CNRS, Villeurbanne, France. Solvents quoted in elemental analyses were observed and integrated in the ^1H NMR spectra. The complex $[CpFe(CO)]_2(\mu\text{-}CO)(\mu\text{-}C{=}CH_2)$ (**1a**) was synthesized following a published procedure.[10] Tcne was sublimated before use.

$Cp_2Fe_2(\mu\text{-}CO)(\mu\text{-}dppe)(\mu\text{-}C{=}CH_2)$ (1b). Complex **1a** (0.700 g, 2.0 mmol) and dppe (0.860 g, 2.3 mmol) were refluxed in toluene (50 mL) for 60 h, during which time the solution turned from red-purple to brown. After being cooled to room temperature, the solution was filtered through Celite, the Celite pad washed several times, and the resulting solution evaporated to dryness. The brown solid was then washed with hexanes (20 mL), acetone (the acetone washing is reddish due to unreacted **1a**) (2 × 15 mL), and finally pentane (2 × 15 mL) and dried under vacuum to give brown microcrystals of **1b** (1.110 g; 1.6 mmol; 80%) that were found pure enough for further syntheses. An analytically pure sample was obtained by recrystallization from dichloromethane/hexanes mixtures. Anal. Calcd for $C_{39}H_{36}Fe_2OP_2$: C, 67.5; H, 5.2. Found: C, 67.6; H, 5.3. IR (CH_2Cl_2, cm^{-1}): ν_{CO} 1705 (m-br). ^1H NMR ($CDCl_3$): δ 7.70–7.10 (m, 20 H, C_6H_5), 6.81 (t, $J_{PH} = 3$ Hz, 2 H, $\mu\text{-}C{=}CH_2$), 4.16 (s, 10 H, C_5H_5), 1.4 (m, 4 H, $CH_2\text{–}P{<}$). $^{31}P\{^1H\}$ NMR ($CDCl_3$): δ 69.1 (s). ^{13}C NMR ($CDCl_3$): δ 297.1 (t, $J_{PC} = 15$ Hz, $\mu\text{-}C{=}CH_2$), 288.6 (t, $J_{PC} = 30$ Hz, μ-CO), 138.7–127.6 (m, C_6H_5), 123.6 (t, $J_{CH} = 155$ Hz, $\mu\text{-}C{=}CH_2$), 86.3 (d, $J_{CH} = 176$ Hz, C_5H_5), 20.8 (dt, $J_{PC} = 26$ Hz, $J_{CH} = 132$ Hz), $\text{–}CH_2P{<}$). UV–vis (CH_2Cl_2) [λ_{max}, nm (ϵ, L mol^{-1} cm^{-1})]: 668 (400), 530 (580), 460 (2600), 360 (4400).

$Cp_2Fe_2(\mu\text{-}CO)(\mu\text{-}dppm)(\mu\text{-}C{=}CH_2)$ (1c). This complex was synthesized via the procedure used for **1b**. Starting with 0.500 g (1.4 mmol) of **1a** and 0.650 g (1.7 mmol) of dppm, 0.71 g (1.0 mmol, 75%) of **1c** is obtained after recrystallization. Anal. Calcd for $C_{38}H_{34}Fe_2OP_2$: C, 67.1; H, 5.0; Fe, 16.4. Found: C, 67.4; H, 5.2; Fe, 16.5. IR (CH_2Cl_2, cm^{-1}): ν_{CO} 1705 (br). ^1H NMR ($CDCl_3$): δ 7.45–7.14 (m, 20 H, C_6H_5), 6.58 (t, $J_{PH} = 3.2$ Hz, 2 H, $\mu\text{-}C{=}CH_2$), 4.31 (s, 10 H, C_5H_5), 1.68 (m, 2 H, $CH_2P{<}$). $^{31}P\{^1H\}$ NMR ($CDCl_3$): δ 87.9 (s).

$[CpFe(CO)]_2(\mu\text{-}CO)[\mu\text{-}C{=}CHC(CN){=}C(CN)_2]$ (2a). Complex **1a** (0.191 g, 0.54 mmol) and tcne (0.063 g, 0.49 mmol) were stirred in toluene (35 mL) for 18 h in the dark. The solution turned from red purple to a deep golden red. It was then filtered, concentrated to ca. 15 mL, and set aside to deposit crystals of **2a**. More product was obtained from the mother liquor by adding petroleum ether. Total yield: 0.160 g, 0.35 mmol, 65%. Anal. Calcd for $C_{20}H_{11}Fe_2N_3O_3$: C, 53.0; H, 2.4; N, 9.3. Found: C, 53.1; H, 2.3; N, 9.3. IR (CH_2Cl_2, cm^{-1}): ν_{CN} 2205 (m), ν_{CO} 2015 (s), 1980 (m), 1815 (s-br), $\nu_{C=C}$ 1470 (s), 1460 (s). ^1H NMR (acetone-d_6, 251 K): δ 8.97 (s, 1 H, $\mu\text{-}C{=}CH\text{–}$), 5.39, 5.36 (total 10 H, C_5H_5). ^{13}C NMR ($CDCl_3$, 0.075 M $Cr(acac)_3$): δ 342.6 (μ-C), 259.6 (μ-CO), 207.5, 207 (Fe–CO), 139.3 (d, $J_{CH} = 159$ Hz, $\mu\text{-}C{=}CH\text{–}$), 132.5 ($\mu\text{-}C{=}CHC(CN){=}C(CN)_2$), 114.7, 113.6, 112.8 (CN), 89.6, 89.2 (C_5H_5), 73.6 ($\mu\text{-}C{=}CHC(CN){=}C(CN)_2$). UV–vis ($CH_2Cl_2$) [$\lambda_{max}$, nm ($\epsilon$, L mol^{-1} cm^{-1})]: 660 (1700), 476 (25500), 332 (9400).

Reaction of $Cp_2Fe_2(\mu\text{-}CO)(\mu\text{-}dppe)(\mu\text{-}C{=}CH_2)$ (1b) with tcne To Give 2b and 3b. To a stirred solid mixture of **1b** (0.700 g, 1.00 mmol) and tcne (0.120 g, 1.00 mmol) was added dichloromethane (25 mL). Upon dissolution, the green color of **1b** was replaced by a strong purple-violet color. After 30 min of stirring, the solution was concentrated and chromatographed on a silica gel column. Eluting with a dichloromethane/hexanes mixture (4/1 by volume) gave first a green band immediately followed by a deep violet one. Recrystallization from a dichloromethane/hexanes mixture gave the green μ-allenylidene complex $\mathrm{Cp_2Fe_2}$(μ-CO)(μ-dppe)[μ-C=C=C(CN)$_2$] (**3b**) (0.130 g, 0.17 mmol, 17%) and the violet μ-butadienylidene complex $\mathrm{Cp_2Fe_2}$(μ-CO)(μ-dppe)[μ-C=CHC(CN)=C(CN)$_2$] (**2b**) (0.520 g, 0.60 mmol, 58%). Data for **3b** are as follows. Anal. Calcd for $\mathrm{C_{42}H_{34}Fe_2N_2OP_2}$: C, 66.7; H, 4.5; Fe, 14.8; N, 3.7. Found: C, 66.1; H, 4.5; Fe, 14.8; N, 3.7. IR ($\mathrm{CH_2Cl_2}$, $\mathrm{cm^{-1}}$): ν_{CN} 2200, 2190 (m), $\nu_{\mathrm{C=C=C}}$ 1837 (m), ν_{CO} 1737 (m-br). ^{1}H NMR ($\mathrm{CDCl_3}$): δ 7.62–7.45 (m, 20 H, $\mathrm{C_6}H_5$), 4.39 (s, 10 H, $\mathrm{C_5}H_5$), 1.28 (m, 4 H, CH_2P<). ^{13}C{^{1}H} NMR ($\mathrm{CDCl_3}$, 0.075 M Cr(acac)$_3$): δ 280.2 (t, J_{PC} = 15 Hz, μ-*C*O), 201.2 (s, μ-C=*C*=C(CN)$_2$), 173.1 (t, J_{PC} = 17 Hz, μ-*C*=C=C(CN)$_2$), 138–128 (*C*$_6$H$_5$), 119.3, 117.4 (*C*N), 86.1 (s, *C*$_5$H$_5$), 39.5 (s, μ-C=C=*C*(CN)$_2$), 20.9 (d, J_{PC} = 24 Hz, *C*H$_2$P<). ^{31}P{^{1}H} NMR ($\mathrm{CDCl_3}$): δ 63.6. Data for **2b** are as follows. Complex **2b** was found to crystallize with one molecule of dichloromethane. Anal. Calcd for $\mathrm{C_{44}H_{35}Fe_2N_3OP_2 \cdot CH_2Cl_2}$: C, 61.4; H, 4.2; N, 4.8. Found: C, 61.7; H, 4.3; N, 4.9. IR ($\mathrm{CH_2Cl_2}$, $\mathrm{cm^{-1}}$): ν_{CN} 2195 (m), ν_{CO} 1740 (m-br), $\nu_{\mathrm{C=C}}$ 1445 (s-br). ^{1}H NMR ($\mathrm{CDCl_3}$): δ 9.39 (t, J_{PH} = 1.9 Hz, 1 H, μ-C=C*H*), 7.70–7.20 (m, 20 H, $\mathrm{C_6}H_5$), 4.61 (s, 10 H, $\mathrm{C_5}H_5$), 1.4 (m, 4 H, CH_2P<). ^{31}P{^{1}H}: δ 61.8. ^{13}C NMR ($\mathrm{CDCl_3}$, 0.075 M Cr(acac)$_3$): δ 378.5 (t, J_{PC} = 16 Hz, μ-*C*=CH–), 283.8 (t, J_{PC} = 29 Hz, μ-*C*O), 141.0 (d, J_{CH} = 154 Hz, μ-C=*C*H–), 137.4–128.1 (m, $\mathrm{C_6}H_5$), 121.7 (s, μ-C=CH*C*(CN)=C(CN)$_2$), 117.6, 116.9, 116.2 (s, *C*N), 89.2 (d, J_{CH} = 178 Hz, *C*$_5$H$_5$), 58.3 (s, μ-C=CHC(CN)=*C*(CN)$_2$), 20.8 (dt, J_{PC} = 30 Hz, J_{CH} = 145 Hz, *C*H$_2$P<). UV–vis ($\mathrm{CH_2Cl_2}$) [$\lambda_{\max}$, nm (ε, L mol^{-1} cm^{-1})]: 539 (25 400), 420 (7500), 330 (10 200).

Reaction of $\mathrm{Cp_2Fe_2}$(μ-CO)(μ-dppm)(μ-C=CH$_2$) (1c) with tcne To Give 2c and 3c. Following the procedure used in the case of **1b**, starting with **1c** (0.510 g, 0.75 mmol) and tcne (0.096 g, 0.75 mmol), the green μ-allenylidene complex $\mathrm{Cp_2Fe_2}$(μ-CO)(μ-dppm)[μ-C=C=C(CN)$_2$] (**3c**) (0.052 g, 0.07 mmol, 9%) and the violet μ-butadienylidene $\mathrm{Cp_2Fe_2}$(μ-CO)(μ-dppm)[μ-C=CHC(CN)=C(CN)$_2$] (**2c**) (0.410 g, 0.52 mmol, 70%) were obtained as nice microcrystals. Complex **3c** was not analyzed but was found pure by IR and NMR spectroscopies. Data for **3c** are as follows. IR ($\mathrm{CH_2Cl_2}$, $\mathrm{cm^{-1}}$): ν_{CN} 2200, 2190 (m), $\nu_{\mathrm{C=C=C}}$ 1835 (m), ν_{CO} 1740 (m-br). ^{1}H NMR ($\mathrm{CDCl_3}$): δ 7.5–7.0 (m, 20 H, $\mathrm{C_6}H_5$), 4.53 (s, 10 H, $\mathrm{C_5}H_5$), 1.70 (m, 2 H, >PCH_2P<). ^{13}C{^{1}H} NMR ($\mathrm{CDCl_3}$): δ 282.0 (t, J_{PC} = 15 Hz, μ-*C*O), 199.3 (s, μ-C=*C*=C(CN)$_2$), 176.0 (t, J_{PC} = 19 Hz, μ-*C*=C=C(CN)$_2$), 135.8–128.2 (*C*$_6$H$_5$), 119.4, 117.2 (s, *C*N), 86.3 (s, *C*$_5$H$_5$), 40.4 (s, μ-C=C=*C*(CN)$_2$), 26.1 (t, J_{PC} = 23 Hz, >PCH$_2$P<). ^{31}P{^{1}H} NMR ($\mathrm{CDCl_3}$): δ 82.4. Data for **2c** are as follows. Anal. Calcd for $\mathrm{C_{43}H_{33}Fe_2N_3OP_2}$: C, 65.6; H, 4.2; N, 5.4. Found: C, 65.6; H, 4.5; N, 5.5. IR ($\mathrm{CH_2Cl_2}$, $\mathrm{cm^{-1}}$): ν_{CN} 2195 (s), ν_{CO} 1755 (m-br), $\nu_{\mathrm{C=C}}$ 1445 (s-br). ^{1}H NMR ($\mathrm{CDCl_3}$): δ 9.32 (t, J_{PH} = 2.2 Hz, 1 H, μ-C=C*H*–), 7.5–7.0 (m, 20 H, $\mathrm{C_6}H_5$), 4.68 (s, 10 H, $\mathrm{C_5}H_5$), 1.75 (m, 2 H, PCH_2P). ^{13}C{^{1}H} NMR ($\mathrm{CDCl_3}$, 0.075 M Cr(acac)$_3$): δ 379.0 (t, J_{PC} = 17 Hz, μ-*C*=CH–), 280.5 (t, J_{PC} = 14 Hz, μ-*C*O), 140.1 (s, μ-C=*C*H–), 135.6–127.6 (m, *C*$_6$H$_5$), 120.8 (s, μ-C=CH-*C*(CN)=C(CN)$_2$), 117.5, 116.6, 115.8 (s, *C*N), 88.8 (s, *C*$_5$H$_5$), 57.7 (s, μ-C=CHC(CN)=*C*(CN)$_2$), 25.2 (t, J_{PC} = 26 Hz, >P*C*H$_2$P<). ^{31}P{^{1}H} NMR: δ 79.6.

$\mathrm{Cp_2Fe_2}$(μ-CO)(μ-dppe)[μ-CCH=C(CN)$_2$]$^+$BF$_4^-$ (4b). Complex **3b** (0.300 g, 0.40 mmol) was dissolved in dichloromethane (20 mL). An excess of $\mathrm{HBF_4 \cdot OMe_2}$ was added dropwise with vigorous stirring at 0 °C. The dark solution was stirred 10 min at room temperature. Half the solvent was then removed under vacuum, and diethyl ether (10 mL) was added to give a precipitate which was washed three times with diethyl ether. The precipitate was dissolved in dichloromethane and the solution filtered through Celite. After washings, the solution was concentrated to ca. 10/15 mL. Diethyl ether (5 mL) was added slowly and the resulting solution stored in a freezer for 3 days to deposit green-brown microcrystals of **4b** that were collected by filtration and dried under vacuum (0.260 g, 0.28 mmol, 70%). These were shown by ^{1}H NMR and elemental analysis to contain $^1/_2$ equiv of dichloromethane. Anal. Calcd for $\mathrm{C_{42}H_{35}BF_4Fe_2N_2OP_2 \cdot {}^1/_2CH_2Cl_2}$: C, 57.6; H, 4.1; N, 3.2. Found: C, 58.2; H, 4.1; N, 3.1. IR ($\mathrm{CH_2Cl_2}$, $\mathrm{cm^{-1}}$): ν_{CN} 2220 (w), ν_{CO} 1785 (s). ^{1}H NMR (acetone-d_6): δ 9.30 (t, 1 H, J_{HP} = 1.9 Hz, μ-CC*H*), 7.8–7.5 (m, 20 H, $\mathrm{C_6}H_5$), 5.26 (d, 10 H, J_{HP} = 1.4 Hz, $\mathrm{C_5}H_5$), 2.2–1.8 (m, 4 H, CH$_2$P<). ^{13}C NMR (acetone-d_6): δ 417.0 (t, J_{PC} = 15 Hz, μ-*C*CH), 266.1 (t, J_{PC} = 13 Hz, μ-*C*O), 190.3 (d, J_{CH} = 157 Hz, μ-C*C*H), 135–124 (m, *C*$_6$H$_5$), 116.4, 114.4 (s, *C*N), 92.2 (d, J_{CH} = 181 Hz, *C*$_5$H$_5$), 63.0 (s, μ-CCH=*C*(CN)$_2$), 22.5 (dt, J_{PC} = 31 Hz, J_{CH} = 134 Hz, *C*H$_2$P<).

Cyclic Voltammetry. The electrochemical experiments were carried out under a nitrogen atmosphere, in carefully deareated dichloromethane with $\mathrm{Bu_4NPF_6}$ as supporting electrolyte. The electrochemical equipment, the cells, and the set of electrodes were as described previously.[44] The potentials in the text, table, and figure are given against ferrocene, which was added as an internal standard at the end of the experiments.

X-ray Analysis of 2a and 3b. Crystals of **2a** and **3b** suitable for X-ray work were obtained by layering with hexanes a concentrated solution of the desired complex in dichloromethane. Intensity data were collected on an Enraf-Nonius CAD-4 automatic diffractometer. Cell dimensions were obtained and refined from a set of 25 high-θ reflections. The scattering factors were taken from ref 45, and the calculations were done according to the SDP package provided by Enraf-Nonius.[46] The weighting scheme used was $w = 1/\sigma(F_o)^2 = [\sigma^2(I) + (0.04F_o^2)^2]^{-1/2}$.

2a. The structure was solved by a combination of Patterson function and Fourier differences. All non-hydrogen atoms were refined anisotropically. Hydrogen atoms were defined between 0.53 and 0.27 e Å^{-3} and refined isotropically. The best full-matrix least-squares refinement of the structure (x, y, z, β_{ij} for non-hydrogen atoms; x, y, z for hydrogen atoms) gave R_w = 0.031 (goodness of fit S_w = 1.27). See Table I for details of the analysis. Positional parameters are given in Table II, and selected bond lengths and angles are provided in Table III.

3b. The structure was solved by direct methods. All non-hydrogen atoms and a $\mathrm{CH_2Cl_2}$ molecule were located after a difference Fourier map. All non-hydrogen atoms expected those of the solvent were refined anisotropically. The majority of hydrogen atoms were defined from a difference Fourier map (0.43–0.12 e Å^{-3}), the others being defined from calculation. The best full-matrix least-squares refinement of the structure (x, y, z, β_{ij} for non-hydrogen atoms; x, y, z, for hydrogen and solvent atoms) gave R_w = 0.045 (goodness of fit S_w = 1.52). See Table I for details of the analysis. Positional parameters are given in Table IV, and selected bond lengths and angles are provided in Table V.

Supplementary Material Available: Tables of general temperature factor expressions, complete positional parameters, and bond lengths and angles including hydrogen atoms (8 pages). Ordering information is given on any current masthead page.

OM9106995

---

(44) Guéguen, M.; Pétillon, F. Y.; Talarmin, J. *Organometallics* **1989**, *8*, 148.

(45) Cromer, D. T.; Waber, J. T. *International Tables for X-Ray Crystallography*; Kynoch Press: Birmingham, U.K., 1975; Vol. IV.

(46) Frenz, B. A. Enraf-Nonius Structure Determination Package; SDP Users Guide. College Station, TX 77840, and Delft, The Netherlands, 1985.